

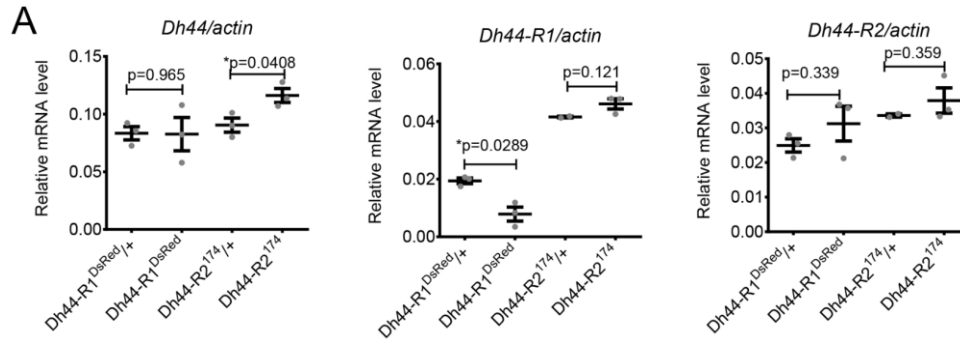
Current Biology, Volume 27

Supplemental Information

A Peptidergic Circuit Links the Circadian

Clock to Locomotor Activity

Anna N. King, Annika F. Barber, Amelia E. Smith, Austin P. Dreyer, Divya Sitaraman, Michael N. Nitabach, Daniel J. Cavanaugh, and Amita Sehgal



B

Dh44-R2 WT	MADDDLRLALV	DSLDDASQED	LAKVIANFSV	DMLQRASALI	GAQQGSSGGQ	LQNRTLQCQQ
Dh44-R2 174	MADDDLRLALV	DSLDDASQED	LAKVIANFSV	DMLQRASALI	GAQQGSSGGQ	LQNRTLQCQQ
Dh44-R2 WT	QQQREEEQAS	LEALASGGKR	ILQCPSSFDS	VLCWPRTNAG	SLAVLPCFEE	FKGVHYDSTD
Dh44-R2 174	QQQREEEQAS	LEALASGGKR	ILQCPSSFDS	VLCWPRTNAG	SLAVLPCFEE	FKGVHYDSTD
Dh44-R2 WT	NATRFVCFPNG	TWDHYSYDR	CHQNSGSIPV	VPDFSPNVEL	PAIYAGGYF	LSFATLVVAL
Dh44-R2 174	NATRFVCFPNG	TWDHYSYDR	CHQNSGSIPV	VPDFSPNVEL	PAIYAGGYF	LSFATLVVAL
Dh44-R2 WT	IIFLSFKDLR	CLRNTIHANL	FLTYITSALL	WILTLFLQVI	TESSQAGCI	TLVIMFYFY
Dh44-R2 174	IIFLSFKDLR	CLRNTIHANL	FLTYITSALL	WILTLFLQVI	TESGWLHNV	GNHVSVLLPN
Dh44-R2 WT	LTNFFWMFVE	GLYLYTLVQ	TFSSDNISFI	IYALIGWGCP	AVCILVWSIA	KAFAPHLNE
Dh44-R2 174	QLFLDVCVGGP	LSVHAGGANI	LQ*H*			
Dh44-R2 WT	HFNGLEIDCA	WMRESHIDWI	FKVPASLALL	VNLVFLIRIM	WVLITKLRSA	HTLETRQYYK
Dh44-R2 WT	ASKALLVLIP	LFGITYLLVL	TGPEQGISRN	LFEAIRAFLLI	STQGFFVALF	YCFLNSEVRQ
Dh44-R2 WT	TLRHGFTRWR	ESRNIHRNSS	IKNRSTEECV	ICLRPSPHTR	LGSLQRYHSI	DITDFV*

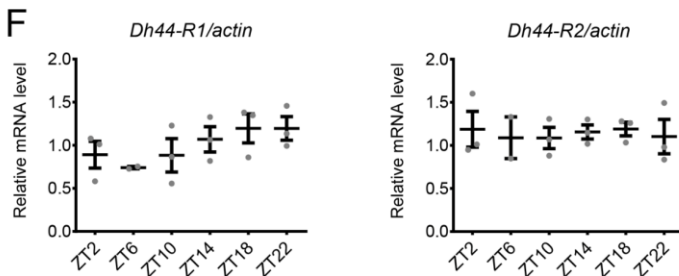
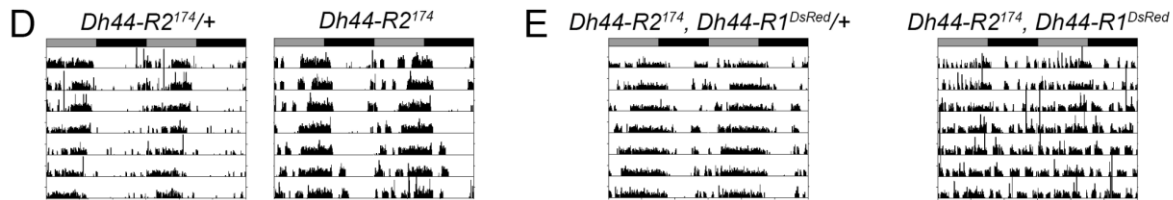
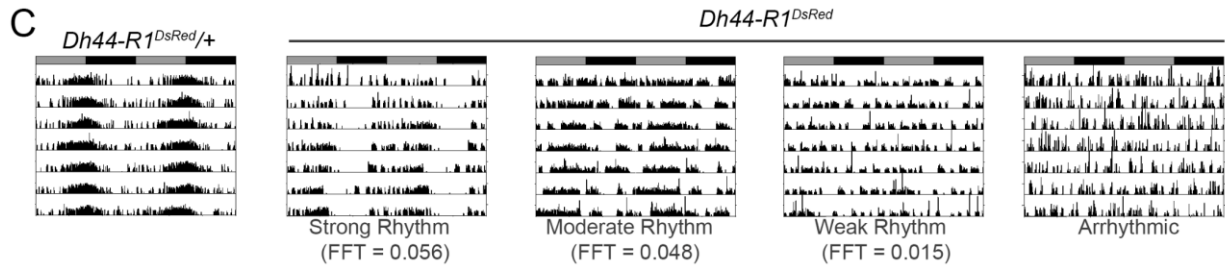


Figure S1. Characterization of Dh44-R1 and Dh44-R2 mutants. Related to Figure 1.

(A) mRNA levels for *Dh44-R1*, *Dh44-R2*, and *Dh44* in whole fly tissue from *Dh44-R1^{DsRed}* and *Dh44-R2¹⁷⁴* mutants. mRNA levels were normalized to *actin* and compared to their heterozygous controls. *P < 0.05 by two-tailed Welch's t-test. qPCR data expressed as mean±SEM from n = 3.

(B) Predicted protein sequences for *Dh44-R2* wild type and *Dh44-R2¹⁷⁴* mutant alleles. *Dh44-R2¹⁷⁴* is a frameshift mutation that changes the protein sequence (indicated with bold text) and results in premature stop codons (indicated with *). Hormone binding domain (blue) and 7-transmembrane domain (orange) are annotated from NCBI's Conserved Domain Database [S1].

(C-E) Representative locomotor activity records from individual flies in constant darkness (DD). Records are double-plotted with gray and black bars indicating subjective day and night, respectively.

(C) Locomotor activity of *Dh44-R1^{DsRed/+}* and *Dh44-R1^{DsRed}* mutant flies in DD. Representative activity records show examples of *Dh44-R1^{DsRed}* homozygous mutants with strong, moderate, weak rhythms or arrhythmic behavior.

(D) Locomotor activity of *Dh44-R2^{174/+}* and *Dh44-R2¹⁷⁴* mutant flies in DD.

(E) Locomotor activity of *Dh44-R2¹⁷⁴, Dh44-R1^{DsRed/+}* and *Dh44-R2¹⁷⁴, Dh44-R1^{DsRed}* double mutant flies in DD.

(F) *Dh44-R1* or *Dh44-R2* mRNA levels in fly head tissue at time points across the day. One-way ANOVA detects no difference between time points (*Dh44-R1*: $F_{5, 11} = 1.27$, P = 0.343; and *Dh44-R2*: $F_{5, 11} = 0.09308$, P = 0.992).

JTK_Cycle [S2] does not detect cycling (*Dh44-R1*: P = 0.272; and *Dh44-R2*: P = 1). mRNA levels were normalized to *actin* levels. qPCR data expressed as mean±SEM from n = 2–3 biological replicates.

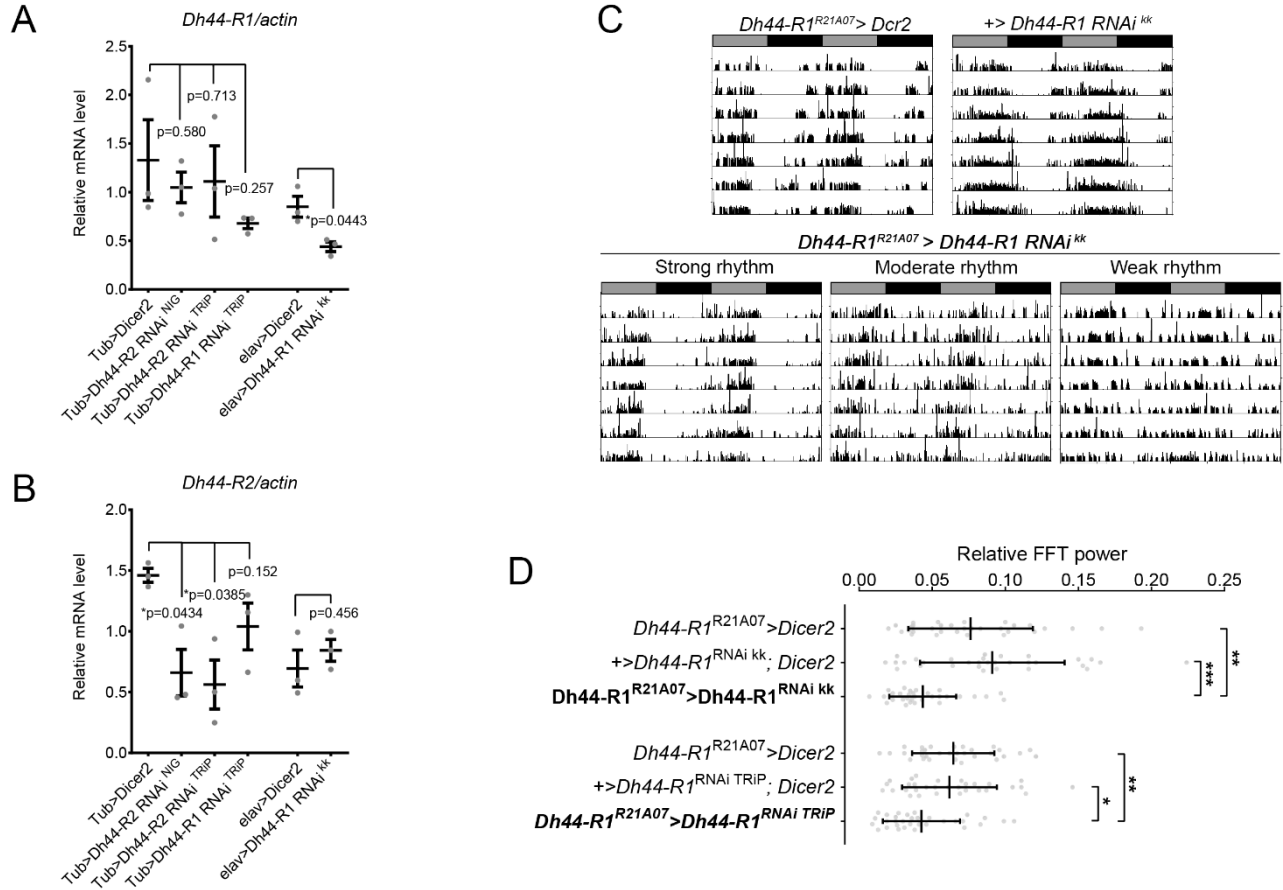


Figure S2. Analysis of RNAi-mediated knockdown of *Dh44-R1*. Related to Figure 1.

(A-B) *Dh44-R1* (A) and *Dh44-R2* (B) mRNA levels in whole fly tissue after knockdown of *Dh44-R1* or *Dh44-R2* using *tubulin-GAL4* (*Tub*) or *elav-GAL4*. mRNA levels were normalized to *actin* and compared relative to GAL4>*Dicer2* control. *Dh44-R1^{RNAi} ^{kk}* knockdown with *Tub-GAL4* was lethal. * $P < 0.05$ by two-tailed Welch's t-test. qPCR data expressed as mean \pm SEM from $n = 3$.

(C) Representative activity records show strong knockdown flies (*Dh44-R1^{R21A07}>Dh44-R1 RNAi^{kk}*) can have strong, moderate, or weak rhythms. Control flies (*Dh44-R1^{R21A07}>Dcr2* or *+>UAS-Dh44-R1 RNAi^{kk}*) have strong rest:activity rhythms.

(D) DD amplitude of rest:activity rhythms represented by FFT analysis in the circadian range. RNAi-mediated knockdown of *Dh44-R1* in *Dh44-R1*-expressing cells lowered the amplitude of rest:activity rhythms in flies (* $P < 0.05$, ** $P < 0.01$, *** $P < 0.001$ by One-way ANOVA with Sidak's multiple comparison test).

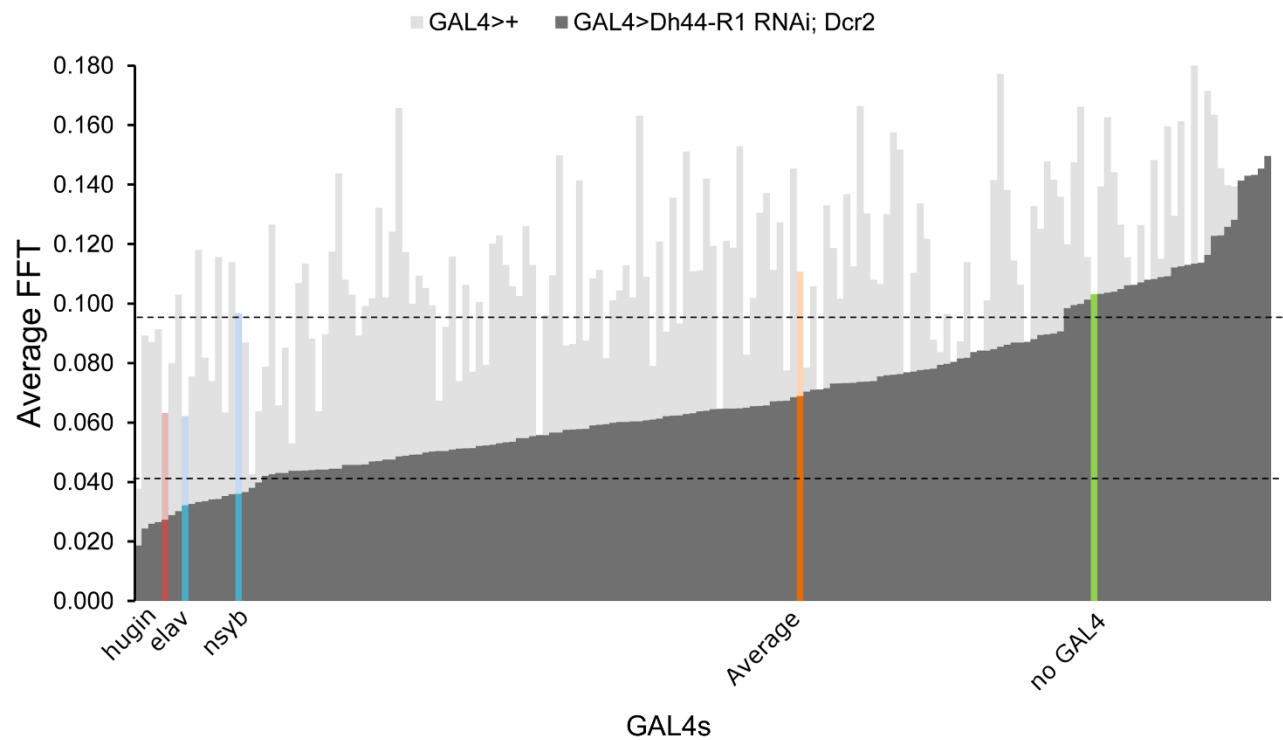


Figure S3. A GAL4 screen with RNAi identifies cells requiring DH44-R1 for strong rest:activity rhythms.

Related to Figure 2.

The mean FFT values for activity rhythms from flies carrying different GAL4 drivers along with *UAS-Dicer2*; *UAS-Dh44-R1^{RNAi^{kk}}* to knock down DH44-R1 (knockdown, dark gray) or the GAL4 alone (negative control, light gray). The average FFT values from all 168 GAL4 tested (orange), no GAL4 control (*UAS-Dicer2*; *UAS-Dh44-R1^{RNAi^{kk}}*; green), and pan-neuronal GAL4s (blue) are shown. Dashed lines denote 1 standard deviation below and above the average FFT from all 168 GAL4 tested. n = 8-16 flies/GAL4, except n = 190 flies for no GAL4 control.

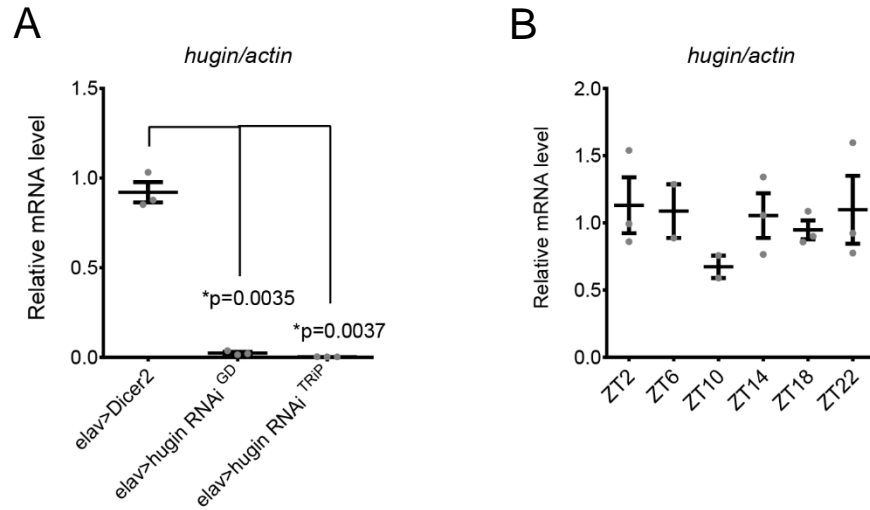


Figure S4. mRNA levels of *hugin* do not cycle across the day. Related to Figures 4 and 5.

(A) *hugin* mRNA levels in whole fly tissue after knockdown of *hugin* using *elav*-GAL4 coupled with *Dicer2* to drive RNAi expression. mRNA levels were normalized to *actin* and compared relative to *elav*-GAL4>*Dicer2* control.

*P<0.01, two-tailed Welch's t-test.

(B) Expression profiling of *hugin* mRNA levels across the day in fly head tissue. One-way ANOVA detects no difference between time points ($F_{5, 10} = 0.6927$, $P = 0.641$). JTK_Cycle does not detect significant cycling ($P = 1$). mRNA levels normalized to *actin*. All qPCR data expressed as mean±SEM from n = 2-3 biological replicates.

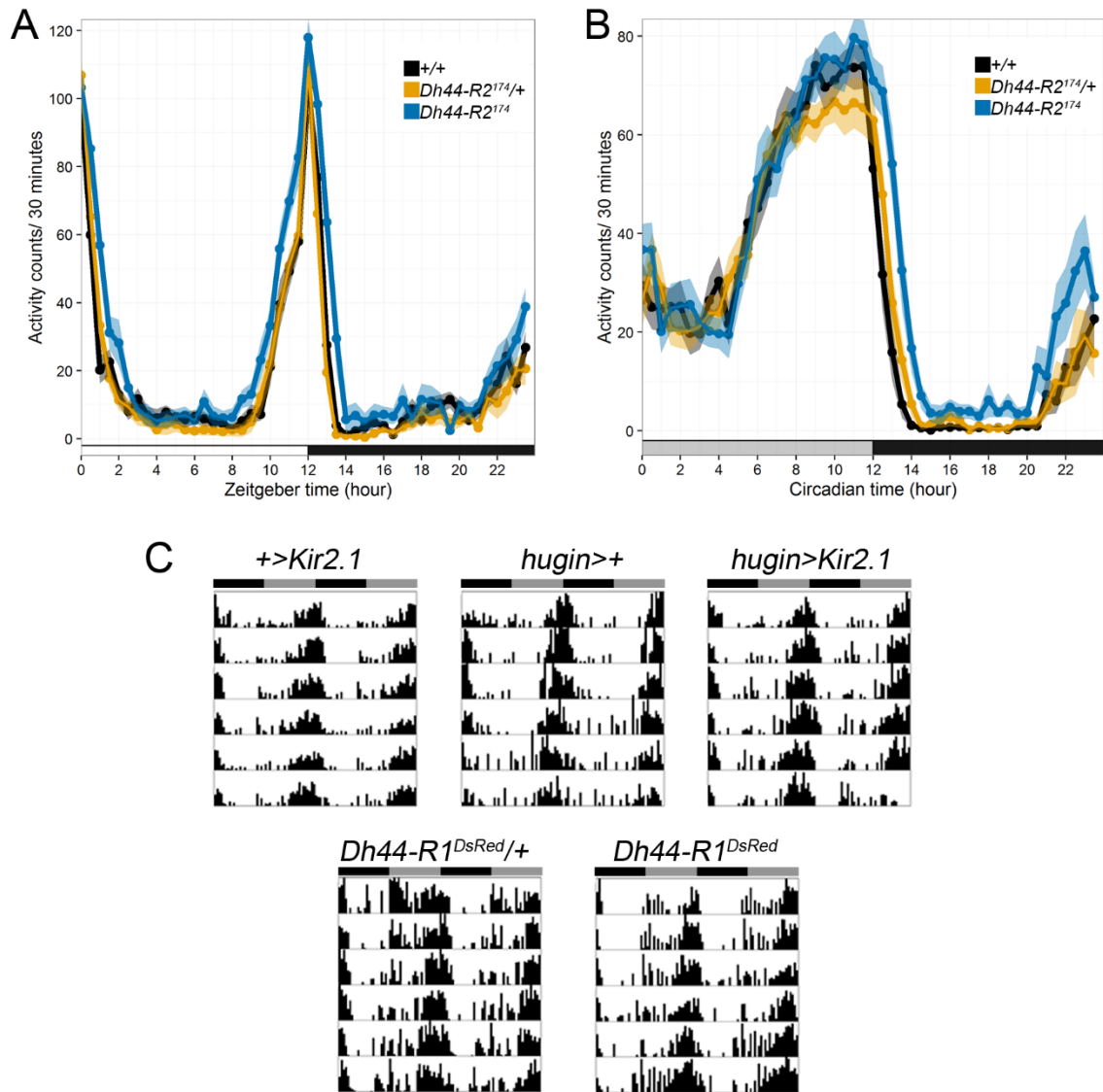


Figure S5. Analysis of locomotor activity and feeding rhythms. Related to Figure 6.

(A-B) Locomotor activity profile of *Dh44-R2¹⁷⁴* mutants averaged over 3 d in LD (A) or 3 d in DD (B). n=15 flies/genotype. Mean \pm SEM

(C) Representative plots of feeding activity for *+>Kir2.1*, *hugin>+*, and *hugin>Kir2.1* flies (top) and *Dh44-R1^{DsRed/+}* and *Dh44-R1^{DsRed}* flies (bottom) in DD. Behavior is double plotted with 6 days of data. Gray and black bars represent subjective day and night, respectively.

Table S1. Analysis of locomotor activity rhythms in flies under DD conditions. Related to Figures 1, 2, and 4.

Table shows number of flies analyzed (*n*), percentages of rhythmic flies (% R), and length of circadian period in hours as mean±SEM. Bold text indicates experimental genotype.

Genotype	n	% R	Period (h) ± SEM
<i>Dh44-R1^{DsRed/+}</i>	44	97.7	23.63 ± 0.04
<i>Dh44-R1^{DsRed}</i>	47	80.9	23.51 ± 0.12
<i>Dh44-R2^{174/+}</i>	47	100	23.75 ± 0.03
<i>Dh44-R2¹⁷⁴</i>	48	95.8	23.91 ± 0.03
<i>Dh44-R2¹⁷⁴, Dh44-R1^{DsRed/+}</i>	48	100	23.61 ± 0.03
<i>Dh44-R2¹⁷⁴, Dh44-R1^{DsRed}</i>	46	93.5	23.39 ± 0.28
<i>Df(2R)BSC700/+</i>	48	100	23.63 ± 0.03
<i>Dh44-R1^{DsRed}/Df(2R)BSC700</i>	47	100	23.53 ± 0.05
<i>Df(2R)BSC305/+</i>	44	100	23.78 ± 0.02
<i>Dh44-R2¹⁷⁴/Df(2R)BSC305</i>	45	97.8	23.56 ± 0.09
<i>pdf⁰¹</i>	46	54.3	22.96 ± 1.05
<i>pdf^{han5304}/Y</i>	47	68.1	22.96 ± 0.62
<i>per⁰¹/Y</i>	46	0	N/A
wild type (<i>w¹¹¹⁸/Y</i>)	46	100	23.73 ± 0.04
<i>elav>UAS-Dicer2</i>	47	97.9	23.41 ± 0.26
<i>+>UAS-Dh44-R1^{RNAi kk}</i>	39	100	23.67 ± 0.07
<i>elav>UAS-Dicer2, UAS-Dh44-R1^{RNAi kk}</i>	30	80	23.46 ± 0.12
<i>+>UAS-Dh44-R1^{RNAi TRiP/+}</i>	45	97.8	23.45 ± 0.08
<i>elav>UAS-Dicer2, UAS-Dh44-R1^{RNAi TRiP}</i>	45	88.9	23.44 ± 0.13
<i>+>UAS-Dh44-R2^{RNAi TRiP}</i>	46	95.7	23.51 ± 0.07
<i>elav>UAS-Dicer2, UAS-Dh44-R2^{RNAi TRiP}</i>	47	74.5	23.42 ± 0.13
<i>+>UAS-Dh44-R2^{RNAi NIG}</i>	48	100	23.91 ± 0.04
<i>elav>UAS-Dicer2, UAS-Dh44-R2^{RNAi NIG}</i>	47	93.6	23.93 ± 0.14
<i>+>UAS-Dh44-R1^{RNAi kk}, UAS-Dh44-R2^{RNAi NIG}</i>	40	97.5	23.82 ± 0.05
<i>elav>Dicer2, Dh44-R1^{RNAi kk}, Dh44-R2^{RNAi NIG}</i>	39	84.6	23.63 ± 0.09
<i>Dh44-R1^{R21A07}>UAS-Dicer2</i>	31	100	23.87 ± 0.06
<i>+>UAS-Dh44-R1^{RNAi kk}</i>	32	100	23.40 ± 0.04
<i>Dh44-R1^{R21A07}>UAS-Dicer2, UAS-Dh44-R1^{RNAi kk}</i>	31	96.8	23.25 ± 0.07
<i>Dh44-R1^{R21A07}>UAS-Dicer2</i>	31	100	23.87 ± 0.04
<i>+>UAS-Dh44-R1^{RNAi TRiP}</i>	31	100	23.37 ± 0.06
<i>Dh44-R1^{R21A07}>UAS-Dicer2, UAS-Dh44-R1^{RNAi TRiP}</i>	31	96.9	23.81 ± 0.06
<i>+>UAS-TrpA1/+ (21°C)</i>	31	100	23.64 ± 0.09
<i>+>UAS-TrpA1/+ (28°C)</i>	31	100	23.68 ± 0.15
<i>Dh44-R1^{R21A07}-GAL4>+ (21°C)</i>	32	96.9	23.91 ± 0.33
<i>Dh44-R1^{R21A07}-GAL4>+ (28°C)</i>	32	100	23.70 ± 0.23
<i>Dh44-R1^{R21A07}>UAS-TrpA1 (21°C)</i>	31	93.5	23.70 ± 0.18
<i>Dh44-R1^{R21A07}>UAS-TrpA1 (28°C)</i>	31	31	23.39 ± 0.08
<i>Dh44-R1^{DsRed/+}; hugin>UAS-Dicer2</i>	30	100	23.53 ± 0.04
<i>Dh44-R1^{DsRed/+}; +>UAS-Dh44-R1^{RNAi kk}</i>	32	100	23.24 ± 0.33
<i>Dh44-R1^{DsRed/+}; hug>UAS-Dicer2, UAS-Dh44-R1^{RNAi kk}</i>	29	96.6	23.80 ± 0.45
<i>Dh44-R1^{DsRed/+}; +>UAS-Dh44-R1^{RNAi TRiP/+}</i>	24	95.8	23.78 ± 0.05
<i>Dh44-R1^{DsRed/+}; hug>UAS-Dicer2, UAS-Dh44-R1^{RNAi TRiP}</i>	19	78.9	23.67 ± 0.19

+>UAS- <i>t-Dh44</i>	62	100	23.56 ± 0.05
<i>hugin</i> -GAL4>+	61	100	23.58 ± 0.03
<i>hugin</i>>UAS-<i>t-Dh44</i>	60	96.8	23.50 ± 0.07
<i>hugin</i> -GAL4>+	32	100	23.64 ± 0.04
+>UAS- <i>Kir2.1</i>	32	100	23.47 ± 0.05
<i>hugin</i>>UAS-<i>Kir2.1</i>	31	96.8	23.39 ± 0.07
+>UAS- <i>reaper</i>	32	100	23.83 ± 0.03
<i>hugin</i>>UAS-<i>reaper</i>	31	90.3	23.81 ± 0.06
<i>hugin</i> >UAS- <i>Dicer2</i>	47	100	24.02 ± 0.04
+>UAS- <i>hugin</i> ^{RNAI TRIP}	47	100	23.45 ± 0.04
<i>hugin</i>>UAS-<i>Dicer2</i>, UAS-<i>hugin</i>^{RNAI TRIP}	48	91.7	23.53 ± 0.05
+>UAS- <i>hugin</i> ^{RNAI GD}	48	100	23.89 ± 0.03
<i>hugin</i>>UAS-<i>Dicer2</i>, UAS-<i>hugin</i>^{RNAI GD}	47	100	23.89 ± 0.02

Table S2. Detailed fly genotypes used in experiments. Related to Figures 1-6 and S1-5.

Figure	Genotype
Figure 1B	w/Y; <i>Dh44-R1^{DsRed}/+</i> w/Y; <i>Dh44-R1^{DsRed}/Dh44-R1^{DsRed}</i> w/Y; <i>Df(2R)BSC700/+</i> w/Y; <i>Dh44-R1^{DsRed}/Df(2R)BSC700</i>
Figure 1C	w/Y; <i>Dh44-R2¹⁷⁴/+</i> w/Y; <i>Dh44-R2¹⁷⁴/Dh44-R2¹⁷⁴</i> w/Y; <i>Df(2R)BSC305/+</i> w/Y; <i>Dh44-R2¹⁷⁴/Df(2R)BSC305</i>
Figure 1D	w/Y; <i>Dh44-R2¹⁷⁴,Dh44-R1^{DsRed}/+</i> w/Y; <i>Dh44-R2¹⁷⁴,Dh44-R1^{DsRed}/ Dh44-R2¹⁷⁴,Dh44-R1^{DsRed}</i>
Figure 1E	w/Y; <i>Dh44-R1^{DsRed}</i> w, <i>per⁰¹/Y</i> w;; <i>pdf⁰</i> w, <i>pdf^{han5304}/Y</i> w/Y <i>iso31</i>
Figure 1F	w, <i>elav-GAL4/Y; UAS-Dicer2/+; +/+</i> w/Y; <i>UAS-Dh44-R1 RNAi kk/+; +/+</i> w, <i>elav-GAL4/Y; UAS-Dicer2/UAS-Dh44-R1 RNAi kk; +/+</i> w/Y; <i>+/+; UAS-Dh44-R1 RNAi TRiP/+</i> w, <i>elav-GAL4/Y; UAS-Dicer2/+; UAS-Dh44-R1 RNAi TRiP/+</i>
Figure 1G	w, <i>elav-GAL4/Y; UAS-Dicer2/+; +/+</i> w/Y; <i>+/+; UAS-Dh44-R2 RNAi NIG/+</i> w, <i>elav-GAL4/Y; UAS-Dicer2/+; UAS-Dh44-R2 RNAi NIG/+</i> w/Y; <i>+/+; UAS-Dh44-R2 RNAi TRiP/+</i> w, <i>elav-GAL4/Y; UAS-Dicer2/+; UAS-Dh44-R2 RNAi TRiP/+</i>
Figure 1H	<i>elav-GAL4/Y; UAS-Dicer2/+; +/+</i> w/Y; <i>UAS-Dh44-R1 RNAi kk/+; UAS-Dh44-R2 RNAi NIG/+</i> <i>elav-GAL4/Y; UAS-Dicer2/UAS-Dh44-R1 RNAi kk; UAS-Dh44-R2 RNAi NIG/+</i>
Figure 1I	w/Y; <i>UAS-GFP.nls/+; Dh44-R1^{R21A07}-GAL4/+</i>
Figure 1J-K.	w/Y; <i>+/+; Dh44-R1^{R21A07}-GAL4/+</i> w/Y; <i>UAS-dTrpA1/+; +/+</i> w/Y; <i>UAS-dTrpA1/+; Dh44-R1^{R21A07}-GAL4/+</i>
Figure 2A	w/Y; <i>UAS-Dh44-R1 RNAi kk/+; UAS-Dicer2/+</i> w/Y; <i>+/+; GAL4/+ or w/Y; GAL4/+; +/+</i> w/Y; <i>UAS-Dh44-R1 RNAi kk/+; UAS-Dicer2/GAL4 or w/Y; UAS-Dh44-R1 RNAi kk/GAL4; UAS-Dicer2/+</i>
Figure 2B	w/Y; <i>UAS-GFP.nls/+; GAL4/+</i>
Figure 2C	w/Y; <i>Dh44-R1^{DsRed}/+; hug-GAL4/UAS-Dicer2</i> w/Y; <i>Dh44-R1^{DsRed}/+,UAS-Dh44-R1 RNAi kk; UAS-Dicer2/+</i> w/Y; <i>Dh44-R1^{DsRed}/+,UAS-Dh44-R1 RNAi kk; hug-GAL4/UAS-Dicer2</i> w/Y; <i>Dh44-R1^{DsRed}/+,UAS-Dicer2; UAS-Dh44-R1 RNAi TRiP/+</i> w/Y; <i>Dh44-R1^{DsRed}/+,UAS-Dicer2; hug-GAL4/UAS-Dh44-R1 RNAi TRiP</i>
Figure 2D	w/Y; <i>UAS-t-Dh44/+</i> w/Y; <i>+/+; hug-GAL4/+</i> w/Y; <i>UAS-t-Dh44/+; hug-GAL4/+</i>
Figure 3B	w/Y; <i>UAS-Denmark,UAS-syt-GFP/+; hug-GAL4/+</i>
Figure 3C	w/Y; <i>UAS-Denmark,UAS-syt-GFP/+; Dh44-GAL4/+</i>

Figure 3D, 3G	<i>w/Y; hug-LexA/LexAop-CD4-spGFP11; Dh44-GAL4/UAS-Nrx-spGFP1-10</i>
Figure 3E.	<i>w/Y; Dh44-LexA/UAS-Denmark; hug-GAL4/LexAop-Rab3-GFP</i>
Figure 3F, H	<i>w/Y; hug-LexA/UAS-Denmark; Dh44-GAL4/LexAop-Rab3-GFP</i>
Figure 3I-J	<i>w/Y; hug-LexA/UAS-P2X2; Dh44-GAL4/LexAop-GCaMP6m-p10</i> <i>w/Y; hug-LexA/UAS-P2X2; Dh44-GAL4/LexAop-GCaMP6m-p10</i> <i>w/Y; hug-LexA/UAS-P2X2; +/-LexAop-GCaMP6m-p10</i>
Figure 3K-M	<i>w/Y; Dh44-R1^{DsRed},UAS-P2X2/Dh44-R1^{DsRed},hug-LexA; Dh44-GAL4/LexAop-GCaMP6m-p10</i> <i>w/Y; Dh44-R1^{DsRed},UAS-P2X2/+,hug-LexA; Dh44-GAL4/LexAop-GCaMP6m-p10</i> <i>w/Y; Dh44-R1^{DsRed},UAS-P2X2/+,hug-LexA; +/-LexAop-GCaMP6m-p10</i>
Figure 4A	<i>w/Y; +/+; hug-GAL4/+</i> <i>w/Y; +/+; UAS-Kir2.1/+</i> <i>w/Y; +/+; hug-GAL4/UAS-Kir2.1</i> <i>yw,UAS-reaper/Y; +/+; +/+</i> <i>yw,UAS-reaper/Y; +/+; hug-GAL4/+</i>
Figure 4B	<i>w/Y; UAS-Dicer2/+; hug-GAL4/+</i> <i>w/Y; +/+; UAS-hugin RNAi TRiP/+</i> <i>w/Y; UAS-Dicer2/+; hug-GAL4/UAS-hugin RNAi TRiP</i> <i>w/Y; +/+; UAS-hugin RNAi GD/+</i> <i>w/Y; UAS-Dicer2/+; hug-GAL4/UAS-hugin RNAi GD</i>
Figure 4C	<i>w/Y; UAS-Denmark,UAS-syt-GFP/+; hug-GAL4/+</i>
Figure 4D	<i>w/Y; hug-LexA,vglut-GAL4/UAS-Denmark; LexAop-Rab3-GFP/+</i>
Figure 4E	<i>w/Y; hug-LexA,vglut-GAL4/LexAop-CD4-spGFP11; UAS-CD4-spGFP1-10/+</i>
Figure 5	<i>w/Y; UAS-ANF-GFP,UAS-myr-RFP/+; hug-GAL4/+</i> <i>w, per⁰¹/Y; UAS-ANF-GFP,UAS-myr-RFP/+; hug-GAL4/+</i>
Figure 6A-B.	<i>w/Y; Df(2R)BSC700/+</i> <i>w/Y;Dh44-R1^{DsRed}/+</i> <i>w/Y;Dh44-R1^{DsRed}/Df(2R)BSC700</i>
Figure 6C, 6D, 6F.	<i>w/Y; +/+; hug-GAL4/+</i> <i>w/Y; +/+; UAS-Kir2.1/+</i> <i>w/Y; +/+; hug-GAL4/UAS-Kir2.1</i>
Figure 6E	<i>w/Y;Dh44-R1^{DsRed}/+</i> <i>w/Y;Dh44-R1^{DsRed}/Dh44-R1^{DsRed}</i>
Figure S1A	<i>w/Y; Dh44-R2¹⁷⁴/+</i> <i>w/Y; Dh44-R2¹⁷⁴/Dh44-R2¹⁷⁴</i> <i>w/Y; Dh44-R1^{DsRed}/+</i> <i>w/Y; Dh44-R1^{DsRed}/Dh44-R1^{DsRed}</i>
Figure S1C	<i>w/Y; Dh44-R1^{DsRed}/+</i> <i>w/Y; Dh44-R1^{DsRed}/Dh44-R1^{DsRed}</i>
Figure S1D	<i>w/Y; Dh44-R2¹⁷⁴/+</i> <i>w/Y; Dh44-R2¹⁷⁴/Dh44-R2¹⁷⁴</i>
Figure S1E	<i>w/Y; Dh44-R2¹⁷⁴,Dh44-R1^{DsRed}/+</i> <i>w/Y; Dh44-R2¹⁷⁴,Dh44-R1^{DsRed}/Dh44-R2¹⁷⁴,Dh44-R1^{DsRed}</i>
Figure S1F	<i>w/Y iso31</i>
Figure S2A-B	<i>w/Y; UAS-Dicer2/+; tubulin-GAL4/+</i> <i>w/Y; UAS-Dicer2/+; tubulin-GAL4/UAS-Dh44-R2 RNAi NIG</i> <i>w/Y; UAS-Dicer2/+; tubulin-GAL4/ UAS-Dh44-R2 RNAi TRiP</i> <i>w/Y; UAS-Dicer2/+; tubulin-GAL4/ UAS-Dh44-R1 RNAi TRiP</i> <i>w,elav-GAL4/Y; UAS-Dicer2/+; +/+</i> <i>w,elav-GAL4/Y; UAS-Dicer2/UAS-Dh44-R1 RNAi kk; +/+</i>

Figure S2C-D	<p>w/Y; +/+; <i>Dh44-R1^{R21A07}-GAL4/UAS-Dicer2</i></p> <p>w/Y; <i>UAS-Dh44-R1 RNAi kk/+; UAS-Dicer2/+</i></p> <p>w/Y; <i>UAS-Dh44-R1 RNAi kk/+; Dh44-R1^{R21A07}-GAL4/UAS-Dicer2</i></p> <p>w/Y; <i>UAS-Dicer2/+; UAS-Dh44-R1 RNAi TRiP/+</i></p> <p>w/Y; <i>UAS-Dicer2/+; Dh44-R1^{R21A07}-GAL4/UAS-Dh44-R1 RNAi TRiP</i></p>
Figure S3	<p>w/Y; <i>UAS-Dh44-R1 RNAi kk/+; UAS-Dicer2/+</i></p> <p>w/Y; +/+; <i>GAL4/+</i> or w/Y; <i>GAL4/+; +/+</i></p> <p>w/Y; <i>UAS-Dh44-R1 RNAi kk/+; UAS-Dicer2/GAL4</i> or w/Y; <i>UAS-Dh44-R1 RNAi kk/GAL4; UAS-Dicer2/+</i></p>
Figure S4A	<p>w,<i>elav-GAL4/Y; UAS-Dicer2/+; +/+</i></p> <p>w,<i>elav-GAL4/Y; UAS-Dicer2/+; UAS-hugin RNAi TRiP/+</i></p> <p>w,<i>elav-GAL4/Y; UAS-Dicer2/+; UAS-hugin RNAi GD/+</i></p>
Figure S4B	w/Y <i>iso31</i>
Figure S5A-B	<p>w/Y <i>iso31</i></p> <p>w/Y; <i>Dh44-R2¹⁷⁴/+; +/+</i></p> <p>w/Y; <i>Dh44-R2¹⁷⁴/Dh44-R2¹⁷⁴; +/+</i></p>
Figure S5C-D	<p>w/Y; +/+; <i>hug-GAL4/+</i></p> <p>w/Y; +/+; <i>UAS-Kir2.1/+</i></p> <p>w/Y; +/+; <i>hug-GAL4/UAS-Kir2.1</i></p> <p>w/Y; <i>Dh44-R1^{DsRed}/+ and w/Y; Dh44-R1^{DsRed}/Dh44-R1^{DsRed}</i></p>

Table S3. Sequences used in generating *Dh44-R1* and *Dh44-R2* CRISPR mutants. Related to STAR Methods.

Primer	Sequence 5' → 3'
gRNA sequences and primers used to generate and screen <i>Dh44-R1</i> and <i>Dh44-R2</i> CRISPR mutations.	
gRNA to exon 6 of <i>Dh44-R2</i>	GATAACCACAGAGTCTAGTC AGG
gRNA to 5' end of <i>Dh44-R1</i>	GTTGTCAATTCGTAGGGAAA TGG
gRNA to 3' end of <i>Dh44-R1</i>	GGGCATTGTTGGAGCCCCGG TGG
Cloning primers for HDR template <i>Dh44-R1</i> ^{DsRed}	
5'HA-Dh44-R1 Forward	CATTGCATGCGTGGAGCACCCAAGCCTTG
5'HA-Dh44-R1 Reverse	TACTGCGGCCCGCCCTACGAATTGACAACG TTC
3'HA-Dh44-R1 Forward	TATAACTAGTGGGCTCCAACAATGCCCTG
3'HA-Dh44-R1 Reverse	AGTGGCGCGCCAAAGAGCCTTTATTACGAAGGAC
Primers for PCR verification of <i>Dh44-R2</i> CRISPR mutation	
Dh44-R2 Po Forward	TCAACGAAGTTTACCTTGCCAATC
Dh44-R2 Pi Forward	GATAACCACAGAGTCTAGTCAGG
Dh44-R2 P Reverse	ATGAGGGCGTAGATAATAAAGC
Primers for PCR verification of <i>Dh44-R1</i> CRISPR mutation	
5'HA Dh44-R1 far Forward	ACGAAGCCGAGCATAACAGTG
5'HA HDR Reverse	CGGTTCGAGGGTTTCGAAATCGATAAG
3'HA HDR Forward	GTGGTTTGTCCAAACTCATC
3'HA Dh44-R1 far Reverse	GAGCGTCGGACCCAATTAGC

Supplemental References

- S1. Marchler-Bauer, A., Derbyshire, M.K., Gonzales, N.R., Lu, S., Chitsaz, F., Geer, L.Y., Geer, R.C., He, J., Gwadz, M., Hurwitz, D.I., *et al.* (2015). CDD: NCBI's conserved domain database. *Nucleic Acids Res.* 43, D222-6.
- S2. Hughes, M.E., Hogenesch, J.B., and Kornacker, K. (2010). JTK_CYCLE: An Efficient Nonparametric Algorithm for Detecting Rhythmic Components in Genome-Scale Data Sets. *J. Biol. Rhythms* 25, 372–380.